

Article

Mapping Irrigated Areas of Ghana Using Fusion of 30 m and 250 m Resolution Remote-Sensing Data

Murali Krishna Gumma ^{1,*}, Prasad S. Thenkabail ², Fujii Hideto ³, Andrew Nelson ¹, Venkateswarlu Dheeravath ⁴, Dawuni Busia ⁵ and Arnel Rala ¹

¹ International Rice Research Institute, Los Baños, 4031, Philippines;

E-Mails: a.nelson@irri.org (A.N.); a.rala@cgiar.org (A.R.)

² Southwest Geographic Science Center, US Geological Survey (USGS), Flagstaff, AZ 86001, USA;

E-Mail: pthenkabail@usgs.gov

³ Japan International Research Center for Agricultural Sciences, 1-1, Ohwashi, Tsukuba 305-8686,

Japan; E-Mail: fhideto@affrc.go.jp

⁴ United Nations Joint Logistic Center, World Food Program (WFP), Juba, South Sudan, Sudan;

E-Mail: vdheeravath@gmail.com

⁵ Ghana Irrigation Development Authority (GIDA), Accra, 00233, Ghana;

E-Mail: busia.nd@gmail.com

* Author to whom correspondence should be addressed; E-Mail: m.gumma@cgiar.org; muraligk5@gmail.com; Tel.: +63-2-580-5600 ext. 2627; Fax: +63-2-580-5699.

Received: 5 February 2011; in revised form: 30 March 2011 / Accepted: 30 March 2011 /

Published: 15 April 2011

Abstract: Maps of irrigated areas are essential for Ghana's agricultural development. The goal of this research was to map irrigated agricultural areas and explain methods and protocols using remote sensing. Landsat Enhanced Thematic Mapper (ETM+) data and time-series Moderate Resolution Imaging Spectroradiometer (MODIS) data were used to map irrigated agricultural areas as well as other land use/land cover (LULC) classes, for Ghana. Temporal variations in the normalized difference vegetation index (NDVI) pattern obtained in the LULC class were used to identify irrigated and non-irrigated areas. First, the temporal variations in NDVI pattern were found to be more consistent in long-duration irrigated crops than with short-duration rainfed crops due to more assured water supply for irrigated areas. Second, surface water availability for irrigated areas is dependent on shallow dug-wells (on river banks) and dug-outs (in river bottoms) that affect the timing of crop sowing and growth stages, which was in turn reflected in the seasonal NDVI pattern. A decision tree approach using Landsat 30 m one time data fusion with MODIS 250 m

time-series data was adopted to classify, group, and label classes. Finally, classes were tested and verified using ground truth data and national statistics. Fuzzy classification accuracy assessment for the irrigated classes varied between 67 and 93%. An irrigated area derived from remote sensing (32,421 ha) was 20–57% higher than irrigated areas reported by Ghana's Irrigation Development Authority (GIDA). This was because of the uncertainties involved in factors such as: (a) absence of shallow irrigated area statistics in GIDA statistics, (b) non-clarity in the irrigated areas in its use, under-development, and potential for development in GIDA statistics, (c) errors of omissions and commissions in the remote sensing approach, and (d) comparison involving widely varying data types, methods, and approaches used in determining irrigated area statistics using GIDA and remote sensing. Extensive field campaigns to help in better classification and validation of irrigated areas using high (30 m) to very high (<5 m) resolution remote sensing data that are fused with multi temporal data like MODIS are the way forward. This is especially true in accounting for small yet contiguous patches of irrigated areas from dug-wells and dug-outs.

Keywords: irrigated areas; MODIS; Landsat ETM+; Ghana; NDVI

1. Introduction

Agriculture is Ghana's most important economic sector; more than half of its population depends on agriculture directly and indirectly [1]. Generally, in West Africa, the land is used in a continuum of the whole toposequence with the cultivation of crops from the upland to the valley bottom [2]. The potential for irrigated rice production in the inland valley swamps (IVS) and river flood plains is about 1.9 million ha in Ghana, according to the World Bank's estimate [3]. The potential for full-control irrigation development, based on soil and water availability, is estimated at 346,000 ha [3]. Irrigated areas were estimated to be around 30,900 ha under water management, neglecting inland valleys and wetlands [4]. Data from the Ghana Irrigation Development Authority (GIDA) suggest, however, that the irrigated area under full or partial control is only around 10,000 to 11,000 ha.

In Ghana, land for irrigation has been developed since the 1960s, and the GIDA was established in 1977 for the development, management and extension of services for all national irrigation projects [5]. The activities of small-scale farmers were based on rice and other crops in the 22 irrigated agricultural areas administered by the GIDA. The Irrigation Development Center (IDC) was established in 1991 as a center for improving technology, extension and training of the GIDA. The Japan International Cooperation Agency (JICA) implemented a Mini-Project Technical Cooperation, "Research cooperation in the development of irrigation agriculture," for three years from 1993 to 1995, focused on building the research capacity of IDC. However, agricultural productivity did not improve because of poor water management and farming techniques, insufficient maintenance and management of irrigation facilities, shortage of water and inadequate support services for farmers in the pilot areas. Increasing population has led to expansion of urban/peri-urban agriculture in Ghana [6].

Several studies have been conducted on how to map agricultural areas [7–12] using advanced techniques in satellite image analysis. However, mapping of irrigated areas proved to be a challenge

due to the diverse range of irrigated plot sizes, crops and water sources used by farmers [13,14]. The use of Landsat imagery proved to be fast, cheap and successful in mapping small irrigated areas. This was demonstrated by Draeger [14] in estimating the irrigated land area of the Klamath River basin in Oregon. Thiruvengadachari *et al.* [15] also used Landsat data to identify irrigation patterns in semiarid areas in India and Rundquist *et al.* [16] used these to make an inventory of central pivot irrigation systems in Nebraska. Abderrahman *et al.* [17] mapped the irrigated areas of the severely arid regions of Saudi Arabia using temporal Landsat Multispectral Scanner and Thematic Mapper data while Murthy *et al.* [18] used IRS LISS (Indian Remote Sensing Satellite with Linear Imaging Self-Scanning) data to derive a cropping calendar for a canal operation schedule in India. It was Thenkabail *et al.* [19] who demonstrated the use of time-series coarse-resolution satellite data such as those from the National Oceanic and Atmospheric Administration's (NOAA) Advanced Very High Resolution Radiometer (AVHRR) in mapping irrigated areas over the entire world. The most extensive study of irrigation performance assessment was carried out by Alexandridis *et al.* [20] using NOAA-AVHRR data. They investigated the Indus River basin to identify the irrigated areas and assessed the performance of the irrigation systems. Boken *et al.* [21] also demonstrated the potential of NOAA-AVHRR for estimating irrigated areas of three states of the USA (United States America). Thenkabail *et al.* [22] used Moderate Resolution Imaging Spectroradiometer (MODIS) time-series data to generate LULC and a map of irrigated area for the Ganges and Indus river basins. Over time, the use of various satellite data has evolved along with diverse and novel techniques in analyzing them. Kamthonkiat *et al.* [23] described a technique called peak detector algorithm to discriminate between rainfed and irrigated rice crops in Thailand. Biggs *et al.* [13] used MODIS time series combined with ground truth data, agricultural census data and Landsat Thematic Mapper (TM) data to map surface-water irrigation, groundwater irrigation and rainfed ecosystems of the Krishna River basin in the southern Indian peninsula. Quansah *et al.* [24] stressed the importance of NDVI time series to identify and separate different types of irrigation, including surface water, shallow dug wells, lift irrigation and groundwater irrigation.

The above literature has consistently reported that single-date fine-resolution imagery, acquired at critical growth stages, is sufficient to precisely identify where irrigation was applied, even including minor and informal irrigation. However, it is not adequate to derive the intensity of irrigation and cropping calendar of the crop identified. In contrast, a multi-date time-series coarse-resolution imagery can be used to distinguish the differences between irrigated crop types and to derive the irrigation intensity [15,16,19,22]. Therefore, a methodology to integrate the use of both the fine- and coarse-spatial-resolution data sets must be developed [19]. The gap between the use of fine-resolution satellite data and the use of coarse-resolution satellite data must be bridged. Moreover, the existing methodology must be modified to derive irrigated areas using fine-resolution satellite data.

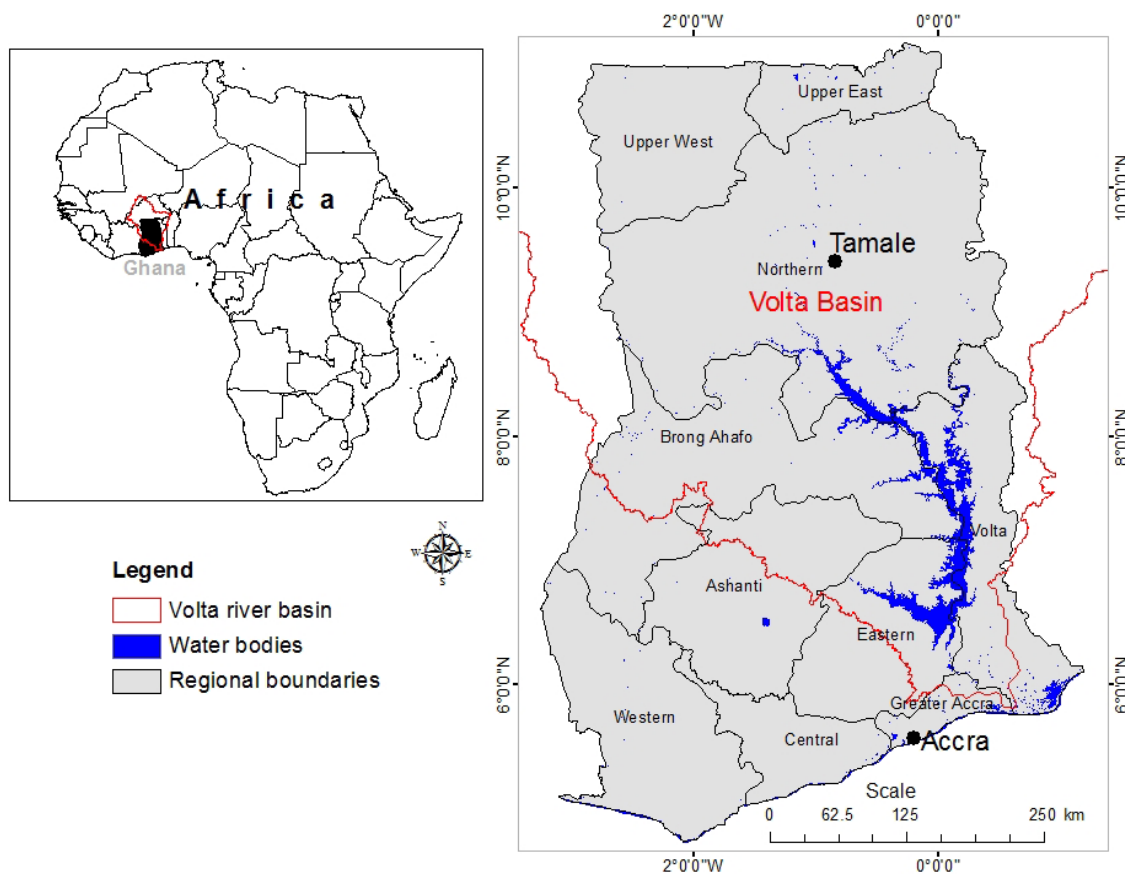
Water use for irrigated agriculture can be determined accurately only from an equally precise estimate of irrigated areas. Precision can be achieved only when discrepancies among area estimates are effectively eliminated. Previous studies have used either only Landsat or only MODIS data for mapping irrigated land. This study aims to map irrigated areas in Ghana using both Landsat ETM+ (from the years 2000 to 2001) and MODIS 250 m data. More specifically, irrigated areas at 30 m resolutions were determined. The whole land area of Ghana was covered by this study. Irrigation types in Ghana vary from large-scale surface water to fragmented and shallow groundwater (along the rivers

and inland valleys). Also, very small fragmented supplemental irrigated areas exist. Climate and elevation vary widely as well. Thus, using finer spatial-resolution data is ideal for mapping irrigated land in Ghana.

2. Study Area

Ghana lies at the shore of the Gulf of Guinea in West Africa and occupies a total area of about 24 million ha (ha). It borders Burkina Faso to the north, Togo to the east and Côte d'Ivoire to the west. The country is divided into ten administrative regions and six ecological zones, dominated by semi-deciduous forest and Guinea savannah (Figure 1).

Figure 1. Study area of Ghana, West Africa, with regions. The figure shows the Volta Basin with provinces. (River basin derived from SRTM 90 m DEM).



The topography is predominantly gently undulating with slopes less than 5%. Rainfall ranges from 700 mm/yr in the coastal zone to 2,200 mm/yr in the southwestern rainforests. Most parts of the country have one distinct rainy season and one dry season lasting longer in the northern parts of Ghana than in the south [25].

About 64% of Ghana's surface lies in the Volta River Basin, Tamale is one of the major cities in the region. Ghana has a population of about 19 million, with an annual growth rate of 2.7%, and its average population density stands at 71 persons/km² and ranges from 20 persons/km² in the north to 900 persons/km² in the capital in the south. Forty-four percent of the population lives in urban areas. The Greater Accra region (hosting the capital city Accra) is the most densely populated and the most

urbanized, as 88% of its almost 3 million people live in the urban areas [26]. Total irrigation potential has been estimated at 1.9 million ha. Another estimate of potential gives 0.7 million ha for small-scale irrigated sawah rice farming (bundling, leveling and puddling fields for irrigated rice cultivation) in inland valley watersheds and, by including the flood plains, this potential could reach 1 million ha [4].

Agriculture is the major source of Ghana's economy. It contributes 36% to the gross domestic product (GDP) and employs 60% of Ghana's labor force [27]. About 36% of Ghana's population lives below the poverty line (US\$1/day) [28]. Poverty is substantially higher in rural areas and in northern Ghana than in urban areas and southern Ghana [26].

3. Data Sets Used for Mapping Irrigated Areas at 30 m

The 30-m Landsat map of irrigated area of Ghana was developed using the following data sets:

3.1. Landsat ETM+ Data

Sixteen Landsat ETM+ tiles were downloaded from the US Geological Survey (USGS), global land cover facility website (<http://edcsns17.cr.usgs.gov/NewEarthExplorer/>). All the images belong to the nominal year 2000 and their spectral characteristics are shown in Table 1. All of them except one tile coincide with the main cropping season. One image over the central part of the basin, coinciding with the non-cropping season, was classified and dealt with separately. All the Landsat ETM+ tiles were converted into reflectance to normalize the multi-date effect [29,30] using a model developed in ERDAS Imagine [31].

Table 1. Characteristics of satellite sensor data used in the study.

Sensor	Spatial (m)	Bands	Band Range (nm)	Irradiance ($\text{W m}^{-2}\text{sr}^{-1}\mu\text{m}^{-1}$)
Landsat ETM+	30	1	0.45–0.52	1,970
		2	0.53–0.61	1,843
		3	0.63–0.69	1,555
		4	0.75–0.90	1,047
		5	1.55–1.75	227
		7	2.09–2.35	1,368
MODIS	250	1	0.62–0.67	1,528
		2	0.84–0.88	974

3.2. MODIS 250-m Data

The MODIS data for Ghana were obtained from NASA [32] and composed data sets from individual images [33]. The 250-m 2-band MODIS data (centered at 648 nm and 858 nm; Table 1) collection 5 (MOD09Q1) were acquired for every 8 days during the crop-growing seasons: June 2000 through May 2001. The data were acquired in 12-bit (0 to 4,096 levels), and were stretched to 16-bit (0 to 65,536 levels). Further processing steps are described in [22,24].

Table 2. Irrigated areas from national statistics (extracted from Ghana Irrigation Development Authority).

Name of scheme	Region	District	Year when construction was completed	No. of households	Irrigation system				
					Potential	Area developed (ha)	Area in use (ha)	Crops	
Anum Valley	Ashanti	Ejisu-Juabeng	1991	115	140	89	0	Pump	Rice, okra, pepper
Akumadan	Ashanti	Offinso North	1976	97	1,000	65	0	Sprinkler	Tomatoes, maize, cowpea
Sata	Ashanti	Sekyerere West	1993	52	56	34	24	Gravity	Okra, maize, cowpea
Subinja	Ashanti	Wenchi	1976	32	121	60	6	Sprinkler	Eggplant, pepper, okra
Okyerako	Central	Gomoa	1976	131	111	81	42	Gravity pump	Rice, chilies, okra
Mankessim	Central	Mfantiman	1978	32	260	17	17	Pump	Watermelon, sweet potato
Amate	Eastern	Amate	1980	127	203	101	0	Gravity pump	Maize, pepper
Dedeso	Eastern	Fanteakwa	1980	69	400	20	8	Sprinkler	Tomato, pepper
Dawhenya	Greater Accra	Dangme West	1978	235	450	200	150	Gravity pump	Rice
Weija	Greater Accra	Kasoa	1984	171	1,500	220	0	Sprinkler	Pepper, tomato, cabbage
Kpong	Greater Accra	Kpong	1968	2,300	3,028	2,786	616	Gravity	Rice, passion fruit
Ashiaman	Greater Accra	Tema	1968	120	155	155	56	Gravity	Rice, maize, pepper, okra
Tanoso	Grong Ahafo	Rechiman	1984	211	115	64	15	Sprinkler	Okra, maize, cowpea
Libga	Northern	Savelugu	1980	41	20	16	16	Gravity	Rice, maize, pepper, okra
Bontanga	Northern	Tolan-Kumbungu	1983	550	570	450	390	Gravity pump	Rice, maize, pepper, okra
Golinga	Northern	Tolan-Kumbungu	1974	80	100	40	16	Gravity	Rice, maize, pepper, okra
Vea (ICOUR)	Upper East	Bolgatanga	1980	2,000	1,197	850	500	Gravity	Rice, tomato, sorghum
Tono (ICOUR)	Upper East	Kassena Nankane	1985	3,250	3,860	2,490	2,450	Gravity	Rice, soybean, tomato
Africa	Volta	Ketu	1983	1,024	950	880	880	Gravity	Rice, okra
Kpando-Torkor	Volta	Kpando	1976	106	356	40	6	Sprinkler	Okra, maize
Aveyime	Volta	North Tongu	1975	83	80	60	0	Gravity pump	Rice
Kikam	Western	Nzema East		22	27	27	0	Pump	Rice
Total				10,848	14,699	8,745	5,192		

3.3. Secondary Data Sets

In addition to Landsat ETM+ and MODIS tiles, the following secondary data sets were used:

3.3.1. SRTM 90-m Elevation

The Shuttle Radar Topography Mission (SRTM) obtained elevation data on a near-global scale to generate the most complete high-resolution digital topographic database of Earth [34,35]. Since the topography of the river basin under investigation is highly diverse, the SRTM elevation data set is useful in separating inland valleys, valley fringes with low elevations and high elevated areas with forest vegetation. The SRTM data (90 m resampled to 30 m) was also used to perform image segmentation based on a drainage network.

3.3.2. Irrigated Areas According to the GIDA

Irrigated area statistics (Table 2) were obtained at the sub-national level (regional level), and represent the total area irrigated by surface water. The data supplied by the GIDA came from the same year (2000-01) as our remote-sensing analysis [26].

4. Methods

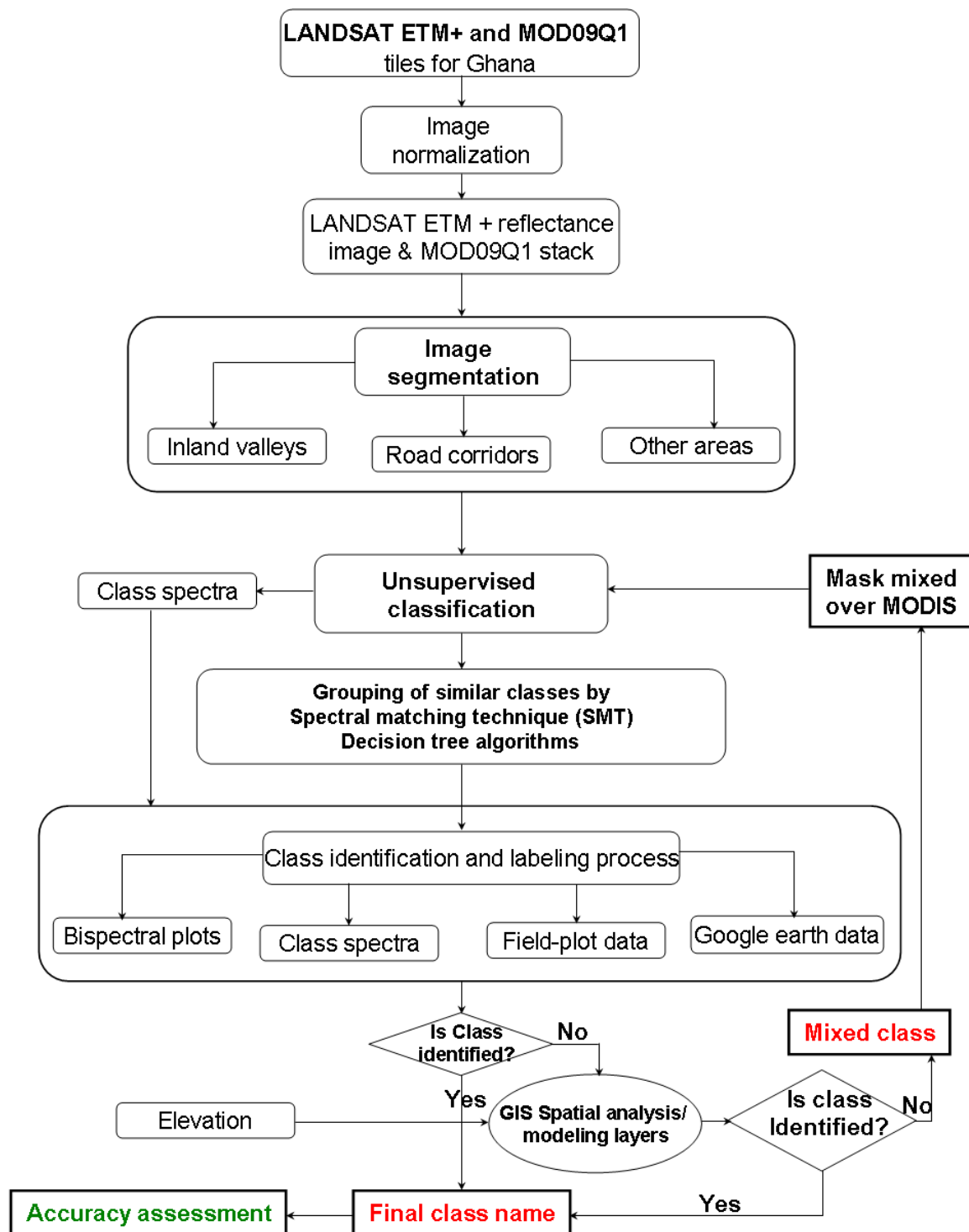
An overview of the comprehensive methodology for mapping irrigated areas using Landsat ETM+ 30 m and MOD09Q1 250 m 8-day time series data presented in Figure 2. The methodology consisted of following steps:

4.1. Image Normalization

The main purpose of this procedure is to normalize the multi-date effect [29,36] of Landsat images for better classification. The Landsat images were converted into top of atmosphere (TOA) reflectance using a reflectance model built in ERDAS Imagine Modeler during this project based on the equations and algorithms presented in [29,36]. The digital number images were first converted to radiance and then to reflectance using the equations given in [29,36]. The meta-data needed for normalization are available in the header files.

4.2. Mega-file Data Cube (MFDC) Creation

A mega-file data cube (MFDC) is akin to hyperspectral data cube. A MFDC consists of a large number of bands in a single file that would help obtain information of all bands with a single click at any point or pixel. Thenkabail *et al.* provide a detailed discussion on MFDC concept [37]. In this study, a MFDC of 51 layers, for a total volume of 35 GB, came from 6 non thermal bands from each of six Landsat ETM+ tiles and 45 NDVI bands from each of four MOD09Q1 tiles. This MFDC covers the entire Ghana for 2000-01 [19] and was analyzed for various segments (Figure 2).

Figure 2. Overview of the methodology for mapping irrigated areas using MODIS data.

4.3. Image Segmentation

The mega-file data cube (MFDC) was divided into three distinct zones (see Figure 2) based on (a) inland valleys, (b) road corridors, and (c) other than these two; the idea behind the segmentation process is to focus more on the segments having higher amounts of agricultural area. Such segments would be classified into more classes than the others for better delineation of different agricultural classes using the protocols presented in Figure 2.

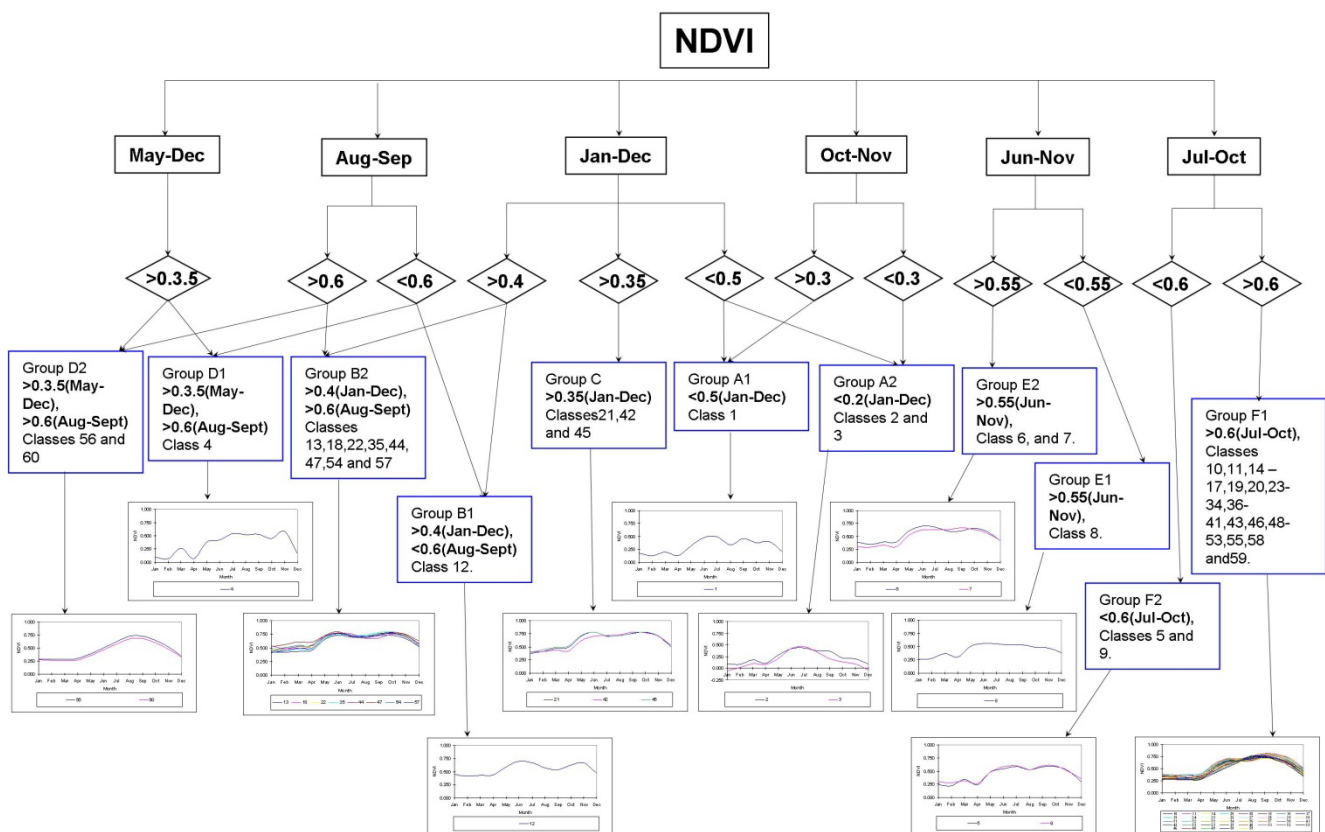
4.4. Classification and Class Spectra Generation

Each segment of Landsat and MODIS MFDC was then classified using unsupervised ISOCCLASS clustering K-means [38]. The number of classes varied from 30 to 100 based on the areas covered by the segment and complexity of the landscape. For example, the inland valley segment was mostly in valley bottoms and valley fringes, and 40 initial classes will be sufficient to determine distinct irrigation types. Since the road corridor segment covered large areas with complex irrigated groundwater and non-irrigated lands, it was classified into 100 classes.

4.5. Grouping of Classes with Decision Tree Algorithms

Decision tree (DT) algorithms [24,39] involve factors such as NDVI, individual band reflectivity, and thermal temperatures to identify and label a class and/or resolve a mixed class. A rule-based DT algorithm (e.g., Figure 3) helps in identifying, grouping, and labeling many classes. However, there are often several classes that remain “mixed”. A class is determined as pure or mixed based on the field-plot data, very high resolution (<5 m) imagery, and bispectral plots (see Section 4.7).

Figure 3. Decision tree algorithm for resolving 60 classes derived from Landsat ETM+ MODIS 250-m data. The Landsat 30-m data were classified along with NDVI spectral signatures generated from the MODIS 250-m time-series data of year 2000-01. This decision tree helped to group the classes into 11 distinct categories.



4.6. Spectral Matching Techniques (SMTs)

Spectral matching techniques (SMTs) match the class spectra derived from classification with an ideal spectra-derived MODIS 250 m MFDC based on precise knowledge of land use from specific locations [40]. Spectral signature matching (SSM) techniques are traditionally developed for hyperspectral data analysis of minerals [40,41]. Time-series data, such as the monthly MODIS NDVI data, are similar to hyperspectral data (12 months in time-series data). These similarities imply that the SMTs, applied for hyperspectral image analysis, also have potential for application in identifying agricultural land use classes from historical time-series satellite imagery.

4.7. Class Identification and Labeling Process

The class identification and labeling process involves the use of the following data sets (Figure 2):

- Bi-spectral plots

The spectral properties of the classes obtained through unsupervised classification were examined on the mega-file using ISODATA statistical cluster algorithm for multi-dimensional data (ERDAS, 2008). The bi-spectral plot for all classes was obtained by plotting the spectral reflectance of Band 3, Red (Landsat), on the x axis and the spectral reflectance of Band 4, near infrared (Landsat), on the y axis [22]. From these plots, the mean NDVI values of the classes were grouped into different clusters based on their spatial location. Each cluster contains classes with more or less identical land cover/land use. Then, each class within a cluster was individually subjected to a process of class identification described in detail by [22].

- Field plot data

A total of 173 field plot points collected across Ghana during several ground truth missions by the International Water Management Institute (IWMI) were used for (a) class identification and (b) accuracy assessments.

- Google Earth data set

Since Google Earth provides very high-resolution images from 30 m to sub-meter resolution for free and accessible through the Web, this data set was also used for class identification and verification, especially to ascertain whether a class is irrigated or rainfed cropland. Though Google Earth does not guarantee pinpoint accuracy, the zoom-in views of high-resolution imagery were used to identify the presence of any irrigation structures (e.g., canals, irrigation channels, open wells). It was observed from the digital globe option on Google Earth that most of the high-resolution imageries were acquired after year 2000 and, on average, Google Earth high-resolution imagery is one to three years old (Google Earth Help). When definitive answers were not available (e.g., absence of irrigation structures), we did not use that particular Google Earth data point in the analysis. Google Earth high-resolution imagery, when used along with other distinct data sets, provides supplemental supportive results.

- MODIS time series

Since the Landsat ETM+ images represent a single-day scenario during the cropping season, MODIS time series (250 m resampled to 30 m) were used to derive the seasonal variations for the same pixel, thus deriving the cropping intensity for each pixel. The classified map is overlaid on the MODIS to derive the statistics. This information is used to build time-series curves for the irrigated pixels. The cropping calendar sequence of the land use is derived from these time-series curves. Annual average NDVI values and timing of the onset of ‘greenness’ are properties of the NDVI time series that allowed separation of land use land cover classes. Annual NDVI in both continuous and double irrigated systems exceeded annual NDVI in rainfed systems, reflecting the higher NDVI in areas irrigated with surface irrigation.

4.8. Resolving the Mixed Classes

The class identification and labeling process (e.g., Figure 3) helps in identifying, grouping, and labeling many classes. However, some complex classes remain unresolved as mixed, as purity of these classes could not be adequately validated using field-plot data and/or very high resolution imagery, and/or bispectral plots, and/or other means. The mixed classes have more than one class in them. For example, some of fragmented shallow groundwater irrigated areas are spectrally (e.g., NDVI, band reflectance) mixed with forest classes. In this study, we found inland valley wetland forest classes, typically had spectral similarity with shallow groundwater irrigated areas. In such cases, we adopted a number of steps to resolve the mixed classes. First, we masked the mixed class and reclassified the class using the mega file data cube covering this mixed class area. Such finer classification on a focused area, helped resolve some mixed classes. Second, we used additional information such as elevation and slope to resolve the mixed classes. For example, irrigated crops are grown in very flat slopes (e.g., valley bottoms) where as inland valley forests are mostly along the valley slopes. Geographic information systems (GIS) spatial modeling approaches were adopted to resolve mixed classes [37]. Overlay, matrix, recode, sieve and proximity analysis [31] based on the theory of map algebra and Boolean logic [42–44] were some of the spatial modeling techniques used. The mixed classes was first masked out from the original Landsat/MODIS data set Together with other spatial data layers (precipitation zones, elevation zones and tree cover categories) and spatial modeling, 5 to 10 or more sub-classes were identified (depending on complexity and area extent). The identification and labeling process as described previously was repeated afterwards (Figure 2).

4.9. Accuracy Assessment

Accuracy was assessed using [45]:

$$A_{ia} = \frac{IFPCIA}{TIFP} \times 100 \quad (1)$$

$$E_c = \frac{NIFPLA}{TNIFP} \times 100 \quad (2)$$

$$E_o = \frac{IFPNIA}{TIFP} \times 100 \quad (3)$$

where

A_{ia} = accuracy of irrigated area classes (percentage)

E_c = errors of commission for the irrigated area class (percentage)

E_o = errors of omission for the irrigated area class (percentage)

IFPCIA = irrigated field plots classified as irrigated areas (number)

TIFP = total irrigated field plots (number)

NIFPIA = non-irrigated field-plot points classified as irrigated areas (number)

TNIFP = total non-irrigated field plots (number)

IFPNIA = irrigated field plots classified as non-irrigated areas (number)

5. Results and Discussions

5.1. Land Use/Land Cover Maps and Area Statistics

Altogether, 12 LULC classes were identified and labeled (Figure 4) based on the above methodology. The LULC areas, including irrigated areas and percentages of total geographical area, are shown in Table 3. The final class name or label (Figure 4, Table 3) is based on the predominance of a particular land use class (e.g., surface irrigation: medium scale, surface water dominant). For example, class 5 in Table 3, “Rainfed croplands, mixed savannas and some barren areas,” is predominantly rainfed cropland during the crop season. Classes 3 and 4 are predominantly located along inland valleys, and they have high water potential for agriculture. Class 6 irrigated areas are predominant in the Greater Accra region and upper eastern part of the study area. Classes 10, 11 and 12 forest classes are predominantly in western, central and Volta regions (Figure 4).

Figure 4. The final 12 LULC classes, including irrigated classes in Ghana, 2000-01.

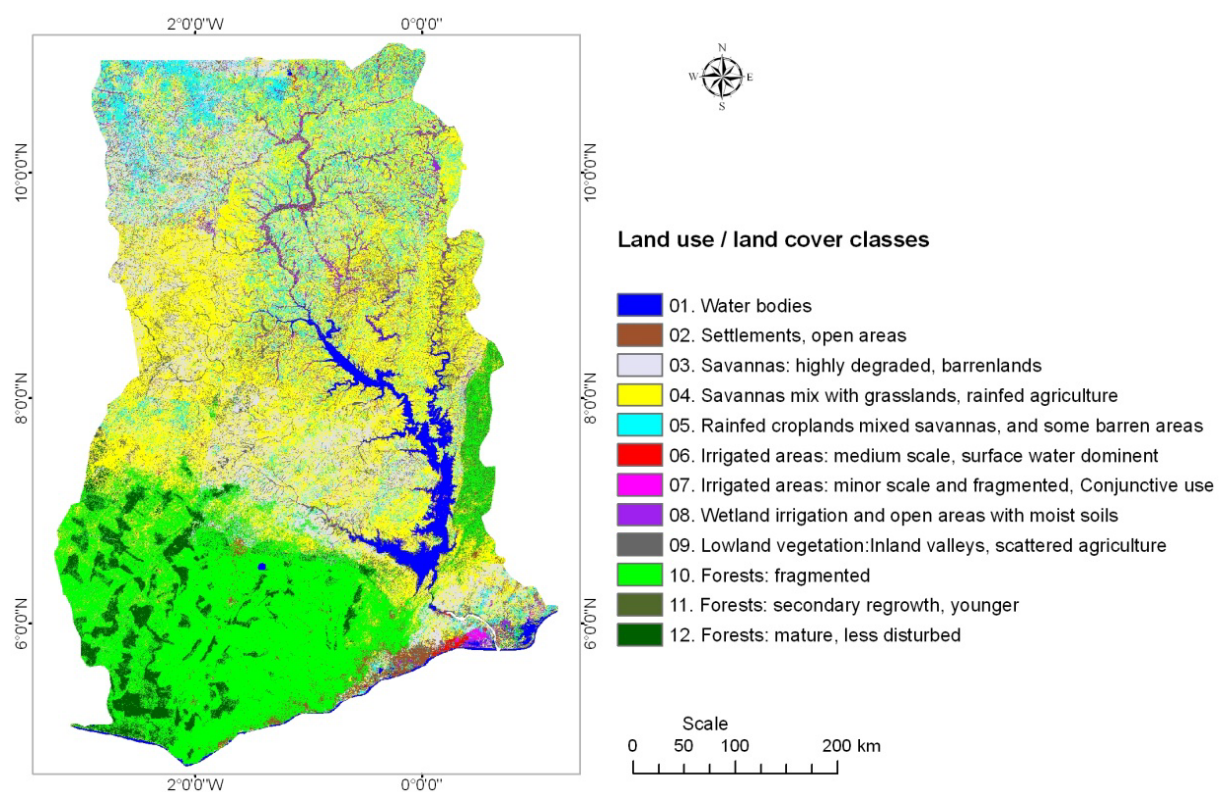


Table 3. Distribution of land use/land cover for the 12 final classes in Ghana.

LULC (no.)	Area (ha)	%
01. Water bodies	765,866	3.2
02. Settlements, open areas	410,984	1.7
03. Savannas: highly degraded, barren lands	3,989,299	16.7
04. Savannas: grasslands, shrub lands, woodlands mixed with rainfed agriculture	7,973,176	33.3
05. Rainfed croplands mixed savannas and some barren areas	2,048,495	8.6
06. Surface irrigation: medium scale, surface water dominant	32,438	0.1
07. Supplemental irrigation: minor scale and fragmented, conjunctive use	181,032	0.8
08. Wetland irrigation and open areas with moist soils	540,814	2.3
09. Lowland vegetation: typically inland valleys, scattered agriculture	1,168,428	4.9
10. Forests: fragmented	5,163,070	21.6
11. Forests: secondary, younger	531,746	2.2
12. Forests: mature, less disturbed	1,110,477	4.6
Total	23,915,825	100

Major irrigated areas were identified in the upper east (northern part) and Greater Accra regions. Minor irrigation areas, including fragmented and conjunctive irrigation (class 7) areas along inland valleys and river corridors, tend to have good water potential for agriculture. Rainfed riparian agricultural areas spread throughout the study area. Wetlands and low land areas were identified in 7.2% of total geographical areas, these areas are highly suitable for rice areas, however inland valleys are rich soils and good ground water potential zones [46].

5.2. Accuracy Assessment

A qualitative accuracy assessment was performed to check whether the irrigated area is classified as irrigated or not, without checking for crop type or type of irrigation, by using equations 1, 2 and 3. The accuracy assessment was performed using field-plot data to derive robust understanding of the accuracies of the data sets used in this study. The field-plot data were based on an extensive field campaign conducted throughout Ghana during the cropping season by International Water Management Institute researchers and they consisted of 173 points. Accuracy assessment provides realistic class accuracies where land cover is heterogeneous and pixel sizes exceed the size of uniform land cover units [13,22,47]. For this study, we had assigned 3×3 cells of Landsat pixels around each of the field-plot points to one of six categories: absolutely correct (100% correct), largely correct (75% or more correct), correct (50% or more correct), incorrect (50% or more incorrect), mostly incorrect (75% or more incorrect), and absolutely incorrect (100% incorrect). Class areas were tabulated for a 3×3 -pixel (9 pixels) window around each field-plot point. If 9 out of 9 Landsat classes matched with field-plot data, this was then labeled absolutely correct and so on (Table 4).

The accuracies and errors of the map of LULC are assessed based on intensive field-plot data (Table 4). The 173 field-plot data points reserved for accuracy assessment from Ghana field campaigns provided a fuzzy classification accuracy of 67–100% for various classes (Table 4).

Table 4. Fuzzy accuracy assessment from field-plot data. Numbers in parentheses indicate the fuzzy correctness percentage. Values in the table indicate the % of field-plot windows in each class with a given correctness percentage.

Land use/land cover (no.)	Sample size (N)	Total correct (%)	Total incorrect (%)	Absolutely correct (100%)	Mostly correct (75% and above)	Correct (51% and above)	Incorrect (51% and above)	Mostly incorrect (75% and above)	Absolutely incorrect (100%)
01. Water bodies	2	100	0	100	0	0	0	0	0
02. Settlements, open areas	5	77	23	55	0	23	23	0	0
03. Savannas: highly degraded, barren lands	55	77	23	55	0	23	23	0	0
04. Savannas: grasslands, shrub lands, woodlands mixed with rainfed agriculture	45	78	22	56	22	0	22	0	0
05. Rainfed croplands, mixed savannas and some barren areas	9	89	11	44	44	0	11	0	0
06. Surface irrigation: medium scale, surface water dominant	7	93	7	86	0	7	7	0	0
07. Supplemental irrigation: minor scale and fragmented, conjunctive use	3	67	33	33	17	17	17	17	0
08. Wetland irrigation and open areas with moist soils	4	75	25	75	0	0	25	0	0
09. Lowland vegetation: typically inland valleys, scattered agriculture	8	94	6	88	0	6	6	0	0
10. Forests: fragmented	22	84	26	14	68	2	2	24	0
11. Forests: secondary, younger	10	90	10	80	0	10	10	0	0
12. Forests: mature, less disturbed	3	67	33	50	0	17	33	0	0
	173	83	18	61	13	9	15	3	0

5.3. Comparisons with National Statistics and Other Studies

The final classified map of irrigated areas was compared against irrigation area statistics obtained from Ghana at the regional level. Data was obtained for 10 major regions. The Landsat and MODIS derived areas consistently over estimated the official estimates in all regions by 20 to 57% (Figure 5(A,B)). The overestimation is obvious in 1:1 plot (Figure 5(C)). The map of irrigated area of Ghana was compared with other studies such as the global irrigated area map (GIAM) [37] and FAO (Table 5).

Figure 5. Comparison of remote sensing derived irrigated areas of Ghana with national statistics: (A) plot without 1 outlier point, (B) plot with outlier point, (C) visual aid to compare the distribution of points against a perfect 1:1 relationship.

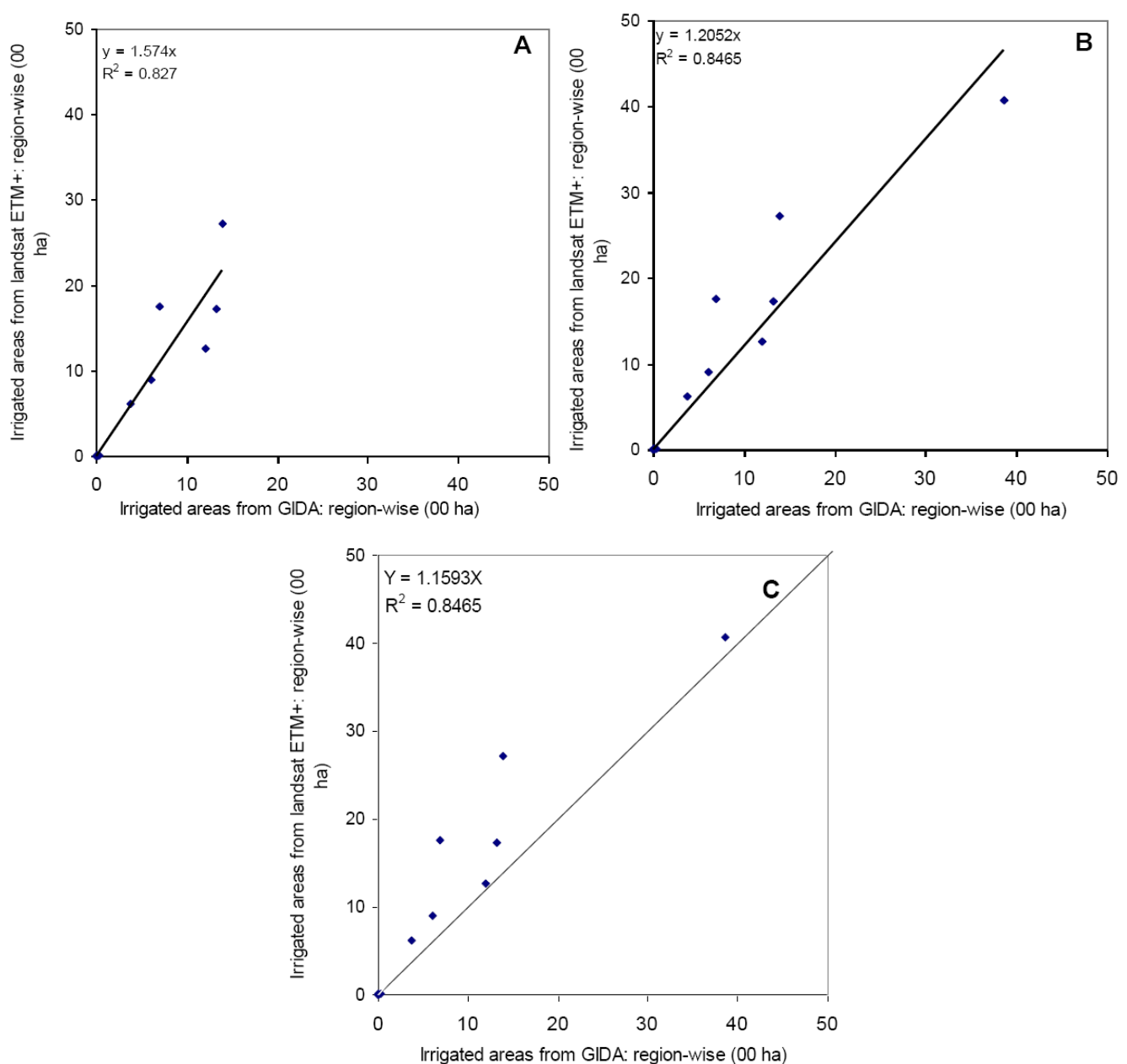


Table 5. The map of irrigated area of Ghana was compared with other studies such as GIAM (global irrigated area map) version 2.0 [44] and FAO.

Source (Spatial Resolution)	Surface Irrigated Area (ha)
¹ Landsat + MODIS (30 m)	32,421
GIAM-V2.0 (AVHRR, 10 km)	28,411
FAO / UF (national reports, 10 km)	30,900

Note: ¹ Present study.

5.4. Effect of Resolution on Irrigated Areas

Ideally, the area under irrigation or any LULC type should be the same irrespective of being mapped by sensors with different resolutions. However, areas determined from sensors with different resolutions often do not match, as reflected in Table 5. High-resolution satellites cover smaller areas, and it is more likely that a single pixel covers a similar LULC class and allows fewer errors in the area estimations. This is why higher and more accurate irrigation areas are obtained using finer spatial resolution. Uncertainties in area calculations are always likely to be higher with coarser resolution imagery. Strong relationships exist in areas between resolutions (Table 5), but often there is a consistent under-estimation of areas in coarser resolution imagery, resulting in smaller irrigation areas.

6. Conclusions

This research combined Landsat ETM+ and MODIS 250 m time-series data with field-plot data to map irrigated areas and other LULC classes in Ghana, which is dominated by smallholder agriculture. The image segmentation approach combined with decision tree algorithm was used to map heterogeneous and patchy irrigated areas, including minor irrigation areas that dominate Ghana's agricultural landscape.

The irrigated area classes were mapped with a fuzzy classification accuracy between 67 and 93%. Overall, irrigated areas were over-estimated by 20 to 57% using remote sensing data, methods, and approaches when compared with Ghana Irrigation Development Authority (GIDA) provincial statistics. Sources of uncertainties include (but not limited to): (a) absence of shallow irrigated area statistics in GIDA statistics, (b) non-clarity in the irrigated areas in its use, under-development, and potential for development in GIDA statistics, (c) errors of omissions and commissions in the remote sensing approach, and (d) comparison involving widely varying data types, methods, and approaches used in determining irrigated area statistics using GIDA and remote sensing.

This study demonstrates significant strengths in using Landsat ETM+ 30 m data (in fusion with time-series MODIS data) in identifying fragmented and minor irrigation sources, such as surface irrigation (large-, medium- and small-scale schemes), inland valleys, and shallow dug wells and dug outs. However, dug-wells, dug-outs, inland valleys, and other fragmented irrigated areas are better mapped using very high resolution (<5 m) data in fusion with time-series coarser resolution data.

Acknowledgments

The authors acknowledge the International Water Management Institute and International Rice Research Institute for providing necessary facilities and infrastructure. This study was financially supported by the Rockefeller Foundation through project number 2008-AGR-305 “*Groundwater in Sub-Saharan Africa: Implications for Food Security and Livelihoods*” Bill and Melinda Gates Foundation project “*Stress- Tolerant Rice for Africa and South Asia*” (STRASA) and by the Ministry of Agriculture, Forestry and Fisheries (MAFF), Japan. The authors would like thank to Bill Hardy, Science Editor/Publisher, IRRI for the excellent editing of grammar and English. The authors would like to thank Alankara Ranjith, IWMI, for editing inland valley boundaries. This paper is not internally reviewed by the US Geological Survey (USGS). Hence, the opinions expressed here are those of the authors and not those of USGS.

References

1. Berry, L.V. Agriculture. In *Ghana: A Country Study*; GPO for the Library of Congress: Washington, DC, USA, 1994. Available online: <http://countrystudies.us/ghana/77.htm> (accessed on 21 May 2010).
2. WARDA. *Training in Rice Production: Instructor’s Manual*; West Africa Rice Development Association: Hong Kong, 1993; p. 290.
3. FAO. *National Aquaculture Sector Overview: Ghana*; Water Resources Research Institute/FAO: Rome, Italy, 2005. Available online: http://www.fao.org/fishery/countrysector/naso_ghana/en (accessed on 21 May 2010).
4. FAO. Ghana. In *Irrigation in Africa in Figures—AQUASTAT Survey 2005*; FAO Water Report No. 29; 2005. Available online: <http://www.fao.org/nr/water/aquastat/countries/ghana/index.stm> (accessed on 21 May 2010).
5. JICA. *The Small-Scale Irrigated Agriculture Promotion Project*; Project Report; Japan International Cooperation Agency: Tokyo, Japan, 2002.
6. Kwasi, A.A. Urban and peri-urban agriculture in developing countries studied using remote sensing and *in situ* methods. *Remote Sens.* **2010**, *2*, 497–513.
7. Ambast, S.K.; Keshari, A.K.; Gosain, A.K. Satellite remote sensing to support management of irrigation systems: Concepts and approaches. *Irrig. Drain.* **2002**, *51*, 25–39.
8. Bastiaanssen, W.G.M.; Molden, D.J.; Thiruvengadachari, S.; Smit, A.A.M.F.R.; Mutuwatte, L.G.J. *Remote Sensing and Hydrologic Models for Performance Assessment in Sirsa Irrigation Circle, India*; International Water Management Institute: Colombo, Sri Lanka, 1999.
9. Ozdogan, M.; Woodcock, C.E.; Salvucci, G.D. Monitoring Changes in Summer Irrigated Crop Area in Southeastern Turkey Using Remote Sensing. In *Proceedings of the 2003 IEEE International Geoscience and Remote Sensing Symposium*, Toulouse, France, 21–25 July 2003; pp. 1570–1572.
10. Sakthivadivel, R.; Thiruvengadachari, S.; Amerasinghe, U.; Bastiaanssen, W.G.M.; Molden, D. *Performance Evaluation of the Bhakra Irrigation System, India, Using Remote Sensing and GIS Techniques*; International Water Management Institute: Colombo, Sri Lanka, 1999.

11. Thiruvengadachari, S.; Sakthivadivel, R. *Satellite Remote Sensing for Assessment of Irrigation System Performance: A Case Study in India*; International Irrigation Management Institute: Colombo, Sri Lanka, 1997.
12. Velpuri, N.M.; Thenkabail, P.S.; Gumma, M.K.; Biradar, C.B.; Noojipady, P.; Dheeravath, V.; Yuanjie, L. Influence of resolution in irrigated area mapping and area estimations. *Photogramm. Eng. Remote Sensing* **2009**, *75*, 1383-1395.
13. Biggs, T.W.; Thenkabail, P.S.; Gumma, M.K.; Scott, C.A.; Parthasaradhi, G.R.; Turrall, H.N. Irrigated area mapping in heterogeneous landscapes with MODIS time series, ground truth and census data, Krishna Basin, India. *Int. J. Remote Sens.* **2006**, *27*, 4245-4266.
14. Draeger, W.C. Monitoring Irrigated Land Acreage Using LANDSAT Imagery: An Application Example. Presented at *Proceedings of the 11th International Symposium on Remote Sensing of Environment*, Ann Arbor, MI, USA, 25–29 April 1977; pp. 515-524.
15. Thiruvengadachari, S. Satellite sensing of irrigation pattern in semiarid areas: An Indian study. *Photogramm. Eng. Remote Sensing* **1981**, *47*, 1493-1499.
16. Rundquist, D.C.; Richardo, H.; Carlson, M.P.; Cook, A. The Nebraska center-pivot inventory—An example of operational satellite remote sensing on a long term basis. *Photogramm. Eng. Remote Sensing* **1989**, *55*, 587-590.
17. Abderrahman, W.A.; Bader, T.A. Remote sensing application to the management of agricultural drainage water in severely arid region: A case study. *Remote Sens. Environ.* **1992**, *42*, 239-246.
18. Murthy, C.S.; Raju, P.V.; Jonna, S.; Hakeem, K.A.; Thiruvengadachari, S. Satellite derived crop calendar for canal operation schedule in Bhadra project command area, India. *Int. J. Remote Sens.* **1998**, *19*, 2865-2876.
19. Thenkabail, P.S.; Biradar, C.M.; Turrall, H.; Noojipady, P.; Li, Y.; Vithanage, J.; Dheeravath, V.; Velpuri, M.; Schull, M.; Cai, X.; Dutta, R. *An Irrigated Area Map of the World (1999) Derived from Remote Sensing*; International Water Management Institute: Colombo, Sri Lanka, 2006.
20. Alexandridis, T.S.A.; Ali, S. *Water Performance Indicators Using Satellite Imagery for the Fordwah Eastern Sadiqia (South) Irrigation and Drainage Project*; International Water Management Institute: Colombo, Sri Lanka, 1999.
21. Boken, V.K.; Hoogenboom, G.; Kogan, F.N.; Hook, J.E.; Thomas, D.L.; Harrison, K.A. Potential of using NOAA-AVHRR data for estimating irrigated area to help solve an inter-state water dispute. *Int. J. Remote Sens.* **2004**, *25*, 2277-2286.
22. Thenkabail, P.S.; Schull, M.; Turrall, H. Ganges and Indus river basin land use/land cover (LULC) and irrigated area mapping using continuous streams of MODIS data. *Remote Sens. Environ.* **2005**, *95*, 317-341.
23. Kamthonkiat, D.; Honda, K.; Turrall, H.; Tripathi, N.K.; Wuwongse, V. Discrimination of irrigated and rainfed rice in a tropical agricultural system using SPOT VEGETATION NDVI and rainfall data. *Int. J. Remote Sens.* **2005**, *26*, 2527-2547.
24. Gumma, M.K.; Thenkabail, P.S.; Iyyanki, M.V.; Velpuri, N.M.; GangadharaRao, T.P.; Dheeravath, V.; Biradar, C.M.; Nalan, S.A.; Gaur, A. Changes in agricultural cropland areas between a water-surplus year and water-deficit year impacting food security determined using MODIS 250m time-series data and spectral matching techniques in the Krishna River Basin (India). *Int. J. Remote Sens.* **2011**, doi: 10.1080/01431161003749485.

25. Quansah, C. Country case study: Ghana. In *Integrated Soil Management for Sustainable Agriculture and Food Security*; FAO-RAF 2000/01; FAO: Accra, Ghana, 2000; pp. 33-75.
26. GSS. *2000 Population and Housing Census*; Summary Report of Final Results; Ghana Statistical Service: Accra, Ghana, 2002.
27. ISSER. *The State of the Ghanaian Economy*; The Institute of Statistical, Social and Economic Research (ISSER), University of Ghana: Legon, Ghana, 2002.
28. Lamptey, N.L. Urban Poverty reduction project launched. *Daily Graphic* 4 March 2006; p. 1.
29. Markham, B.L.; Barker, J.L. *Landsat MSS and TM Post-Calibration Dynamic Ranges, Exoatmospheric Reflectances and At-Satellite Temperatures*; Landsat Technical Notes; Earth Observation Satellite Company: Lanham, MD, USA, 1 August 1986.
30. Thenkabail, P.S.; Enclona, E.A.; Ashton, M.S.; Legg, C.; De Dieu, M.J. Hyperion, IKONOS, ALI, and ETM+ sensors in the study of African rainforests. *Remote Sens. Environ.* **2004**, *90*, 23-43.
31. ERDAS. *ERDAS Field Guide*; ERDAS: Norcross, GA, USA, October 2007; Volume 1.
32. NASA. Moderate Resolution Imaging Spectrometer (MODIS). Available online: <http://modis.gsfc.nasa.gov/> (accessed on 15 August 2007).
33. NASA. MODIS data, Moderate Resolution Imaging Spectrometer (MODIS). Available online: https://lpdaac.usgs.gov/lpdaac/get_data/data_pool (accessed on 15 August 2007).
34. Farr, T.G.M. Kobrick Shuttle Radar Topography Mission produces a wealth of data. *EOS Trans.* **2000**, *81*, 583-585.
35. Rabus, B.; Eineder, M.; Roth, A.; Bamler, R. The shuttle radar topography mission—A new class of digital elevation models acquired by spaceborne radar. *ISPRS J. Photogramm. Eng. Remote Sens.* **2003**, *57*, 241-262.
36. Thenkabail, P.S.; Enclona, E.A.; Ashton, M.S. Hyperion, IKONOS, ALI, ETM+ sensors in the study of African rainforests. *Remote Sens. Environ.* **2004**, *90*, 11.
37. Thenkabail, P.; Biradar, C.; Noojipady, P.; Dheeravath, V.; Li, Y.; Velpuri, M.; Gumma, M.; Reddy, G.; Turrall, H.; Cai, X.; Vithanage, J.; Schull, M.; Dutta, R. Global irrigated area map (GIAM) for the end of the last millennium derived from remote sensing. *Int. J. Remote Sens.* **2009**, *30*, 3679-3733.
38. Tou, J.T.; Gonzalez, R.C. *Pattern Recognition Principles*; Addison-Wesley Publishing Company: Reading, MA, USA, 1975.
39. Defries, R.S.; Hansen, M.C.; Townshend, J.R.G. Global continuous fields of vegetation characteristics: A linear mixture model applied to multi-year 8 km AVHRR data. *Int. J. Remote Sens.* **2000**, *21*, 1389-1414.
40. Thenkabail, P.S.; GangadharaRao, P.; Biggs, T.; Gumma, M.K.; Turrall, H. Spectral Matching Techniques to Determine Historical Land use/Land cover (LULC) and Irrigated Areas using Time-series AVHRR Pathfinder Datasets in the Krishna River Basin, India. *Photogramm. Eng. Remote Sens.* **2007**, *73*, 1029-1040.
41. Homayouni, S.M.R. Material Mapping from Hyperspectral Images Using Spectral Matching in Urban Area. Presented at *the IEEE Workshop in Honour of Professor Landgrebe*, Washington, DC, USA, October 2003.

42. Peuquet, D.; Marble, D. *Introductory Readings in Geographic Information Systems*; Taylor and Francis: New York, NY, USA, 1990; p. 381.
43. Tomlin, C. *Geographic Information Systems and Cartographic Modeling*; Prentice-Hall: Upper Saddle River, NJ, USA, 1990.
44. Tomlinson, R. *Thinking about Geographic Information Systems Planning for Managers*; ESRI Press: Redlands, CA, USA, 2003; p. 283.
45. Congalton, R.G.; Green, K. *Assessing the Accuracy of Remotely Sensed Data: Principles and Practices*; Lewis Publisher: Boca Raton, FL, USA, 1999.
46. Gumma, M.K.; Thenkabail, P.S.; Fujii, H.; Namara, R. Spatial models for selecting the most suitable areas of rice cultivation in the Inland Valley Wetlands of Ghana using remote sensing and geographic information systems. *J. Appl. Remote Sens.* **2009**, *3*, 033537.
47. Gopal, S.; Woodcock, C. Theory and methods for accuracy assessment of thematic maps using fuzzy sets. *Photogramm. Eng. Remote Sensing* **1994**, *60*, 181-188.

© 2011 by the authors; licensee MDPI, Basel, Switzerland. This article is an open access article distributed under the terms and conditions of the Creative Commons Attribution license (<http://creativecommons.org/licenses/by/3.0/>).